SUPPLEMENTARY INFORMATION

TABLE OF CONTENTS:

Supplementary Figures:

Figure S1 ……2
Figure S2 …… 3
Figure S3 …… 4
Figure S4 …… 5
Figure S5 …… 7
Figure S6 …… 8
Figure S7 …… 9
Figure S8 …… 11
Figure S9 …… 14
Figure S10 …… 15
Figure S11 …… 16

SUPPLEMENTARY FIGURES:

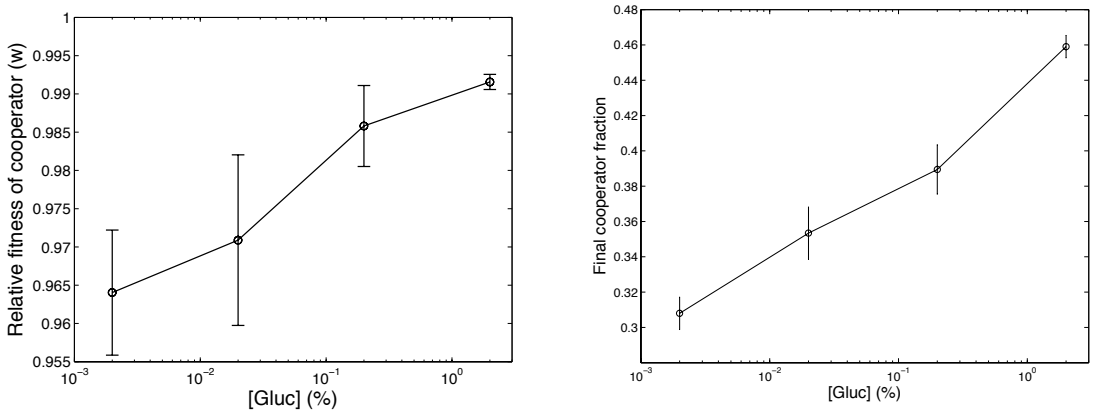

Figure S1: Metabolic cost of invertase production. Invertase expression is maximal at low glucose concentrations but repressed when glucose is abundant(Gancedo, 1998; Ozcan *et al*, 1997). We measured the metabolic cost of invertase production by co-culturing cooperator and mutant cheater yeast strains in media containing only glucose as carbon source, by daily serial dilution (1:1,000) for three days. Starting cooperator fraction was 50% and initial cell density was 1.5×10^5 cells/mL. At high concentrations of glucose, invertase expression is repressed and as expected, there was little fitness difference between the two strains. On the other hand, at low concentrations of glucose where invertase expression reached to its maximum, the cooperator strain had a fitness deficit of ~3-4% consistent with a metabolic cost associated with production and secretion of invertase. Left panel shows the relative fitness (w) values which are calculated using the following expression(Greig & Travisano, 2004):

$$w = \ln\left[\frac{D_f f_f}{D_i f_i}\right] \Big/ \ln\left[\frac{D_f(1-f_f)}{D_i(1-f_i)}\right]$$

where f_i and f_f are the initial and final cooperator fraction and D_f and D_i are the final and initial total cell densities for each day. Right panel shows the final fraction of cooperators in the same experiment after three days of transfers. Data points represent mean of 3 measurements over 3 days with error bars ± s.e.m.

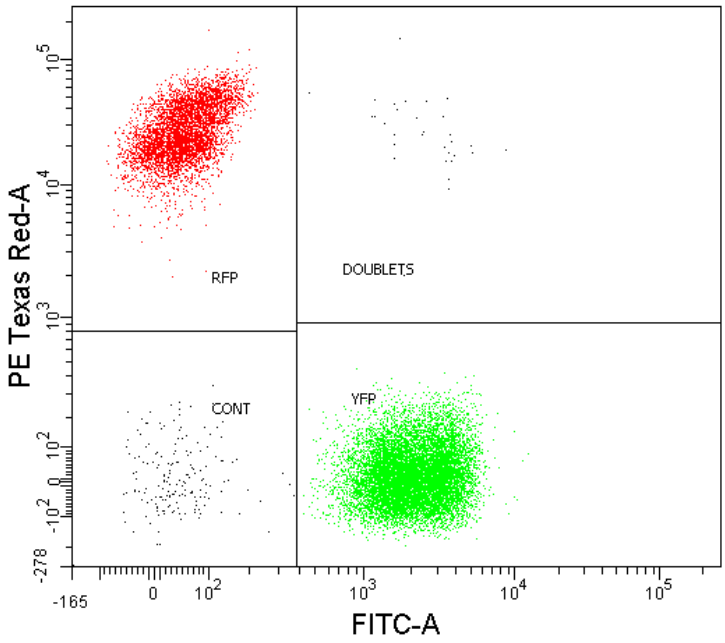

Figure S2: Measurement of cooperator fraction with flow cytometry. Our yeast strains were tagged with constitutively expressed YFP and RFP proteins (cooperator and cheater respectively). We could distinguish between the two strains on BD LSR II flow cytometer. YFP was excited with a blue laser (488 nm) and emission was collected through a 530/30 nm filter (FITC-A channel). RFP was excited with a yellow/green laser (561 nm) and emission was collected through a 610/20 nm filter (PE Texas Red-A channel). The dot plot in the figure is a sample from a competition experiment between yeast and bacteria after 10 days of co-culture. The two strains were well separated on the different fluorescence channels. Cooperator fraction and final yeast density in each well were measured using yeast settings on the flow cytometer (see Methods).

A

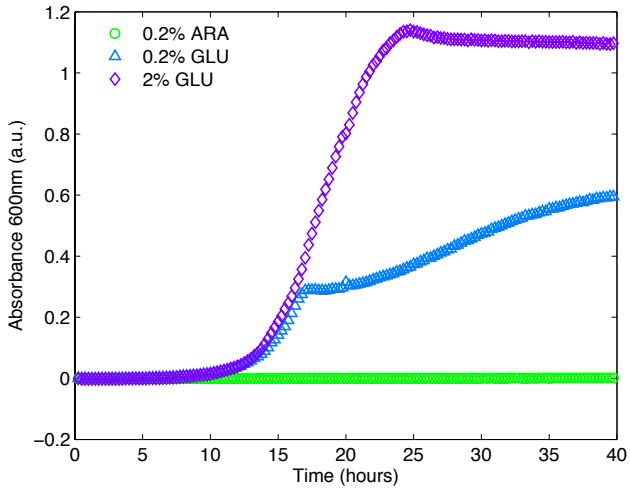

B

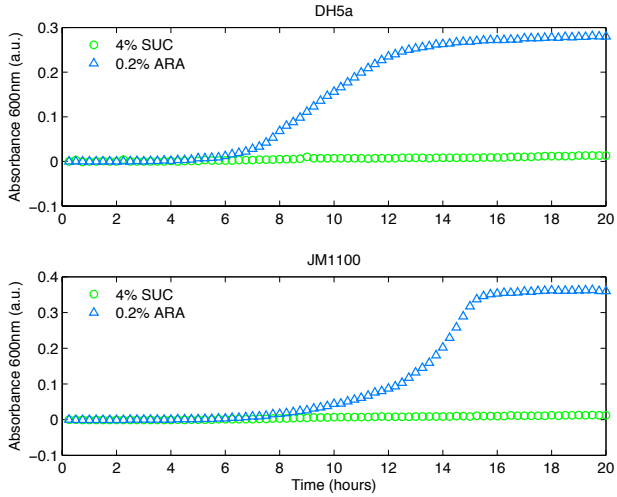

Figure S3: Yeast growth on arabinose and *E.coli* growth on sucrose. (A) We grew yeast (50% cooperator) on 0.2% arabinose, 0.2% glucose or 2% glucose. Initial cell density was the same as in the competition experiments (7.5×10^4 cells/mL). Absorbance at 600 nm was measured for 40 hrs. The results are plotted in the above figure. Our yeast strains were not able to grow on 0.2% arabinose. (B) *E.coli* strains were grown on either 4% sucrose or 0.2% arabinose. Our *E.coli* strains were not able to grow on sucrose.

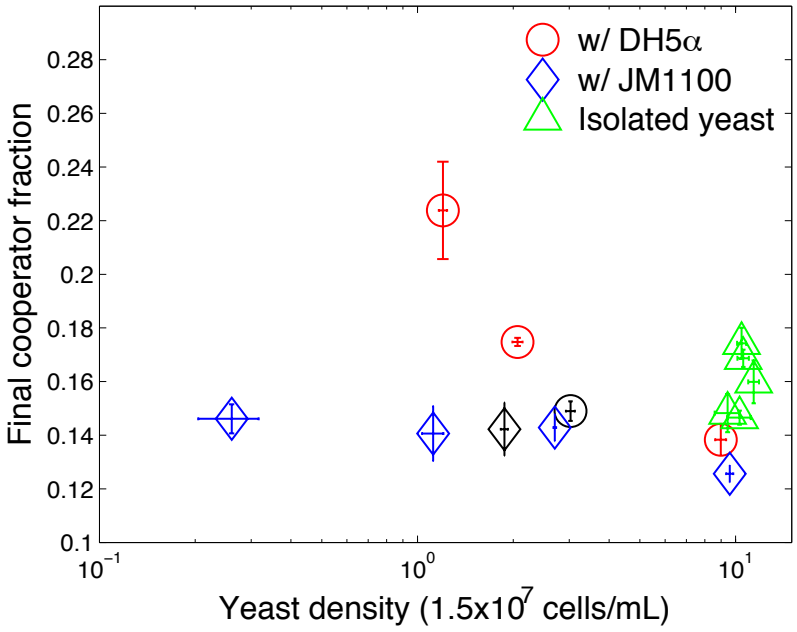

Figure S4: Excess glucose eliminates selection for cooperators in the presence of bacteria. Cooperator fraction after 5 cycles of dilution (10 days of growth) and corresponding final yeast density in competition against bacteria on default media (see Methods). Starting cooperator fraction was 10% for all the data presented. For the conditions with a bacterial competitor (w/ DH5α and w/ JM1100) media contained additional 0.2% glucose. Each individual data point represents the result for a different buffer concentration used. We see that although the yeast density is limited by the presence of bacteria, there is little increase in cooperator fractions when there is excess glucose in the media. Isolated yeast data (triangles) show the highest density yeast population can reach without the presence of bacteria. Black data points are the results for the condition used in figure 1 (4 mM buffering). The reason that the number of data points differ between DH5α and JM1100 treatments is that with DH5α yeast went extinct at some of the highest buffer conditions used and fractions were not calculated for those cases (see Methods).

In addition to these controls, we also tried to grow yeast on media spent by bacteria. To achieve this, we first grew bacteria on default media with varying buffer concentrations. Then, bacteria were spun down and yeast was grown in the supernatant with added glucose (0.2%) for 48 hrs. The results showed no change in the cooperator fraction, again ruling out a fitness difference between our two yeast strains that might be mediated by bacterial resource depletion. However,

we could not dilute and propagate these cultures into new spent media, as the final yeast density was much lower than we observed in our competition experiments. Error bars, ± s.e.m. (n = 3).

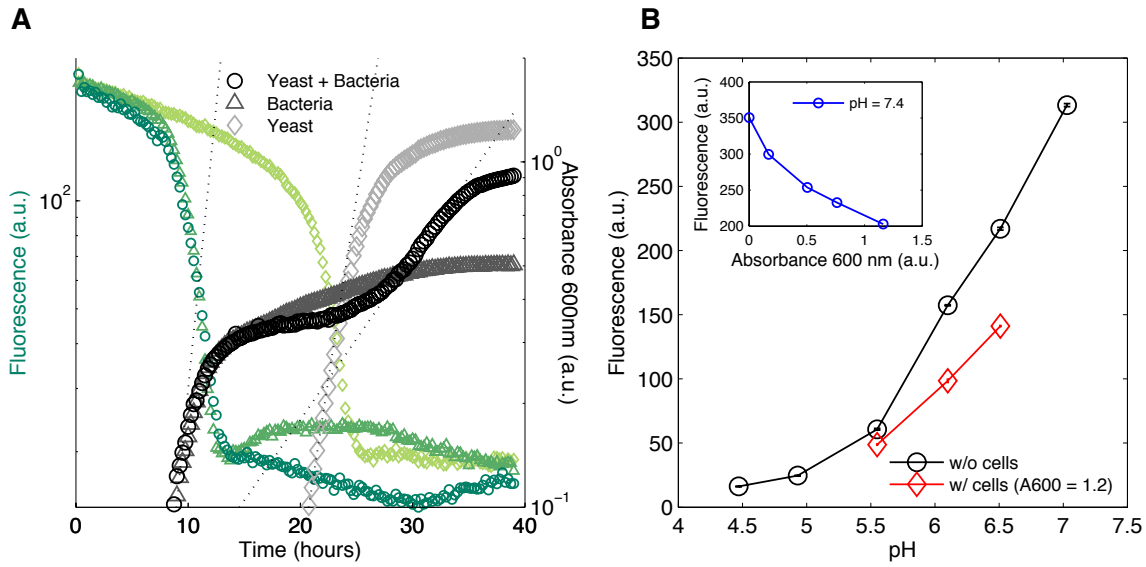

Figure S5. Successional growth dynamics in mixed batch culture. **(A)** Absorbance and fluorescence (~pH, see Methods) measurements for a co-culture of bacteria (DH5α) and yeast, an isolated bacterial culture and an isolated yeast culture. Initial cell densities were as described in Methods and were the same for each species in competition with the other species or by itself. All cultures were buffered with 4 mM PIPES. Dotted lines are the tangents to the absorbance traces during exponential growth. We see that the initial drop in pH in the mixed culture coincides with the pH drop in the isolated bacterial culture, which indicates that initial acidification in the mixed culture is strongly mediated by bacterial fermentation. In contrast, pH drop occurs much later in the isolated yeast culture, as the yeast population takes longer to establish. **(B)** Fluorescein vs. pH calibration curve with and without cells in the media. pH of our default media was adjusted using NaOH without any added buffer and fluorescence was measured as described in Methods. Fluorescein was fluorescent across the relevant pH range (~4.5 to 6.5) and lost its fluorescence completely around pH 4.5, which is also quite close to the pH value where bacterial growth is limited(Foster, 2004). The drop in pH shown in (a) and figure 2a is not due to accumulating cell mass obscuring fluorescence measurement. By suspending yeast cells in the media at a density of 15×10^7 cells/mL (A_{600} ~ 1.2) – which is the maximum density we observed in our experiments – we show that although there is a drop in fluorescence due to the presence of cells, it is not as dramatic as measured during growth. Inset shows the fluorescence versus absorbance (~cell density) relationship measured by suspending yeast cells in PBS (pH = 7.4) at different densities. Error bars, ± s.e.m. (n = 3).

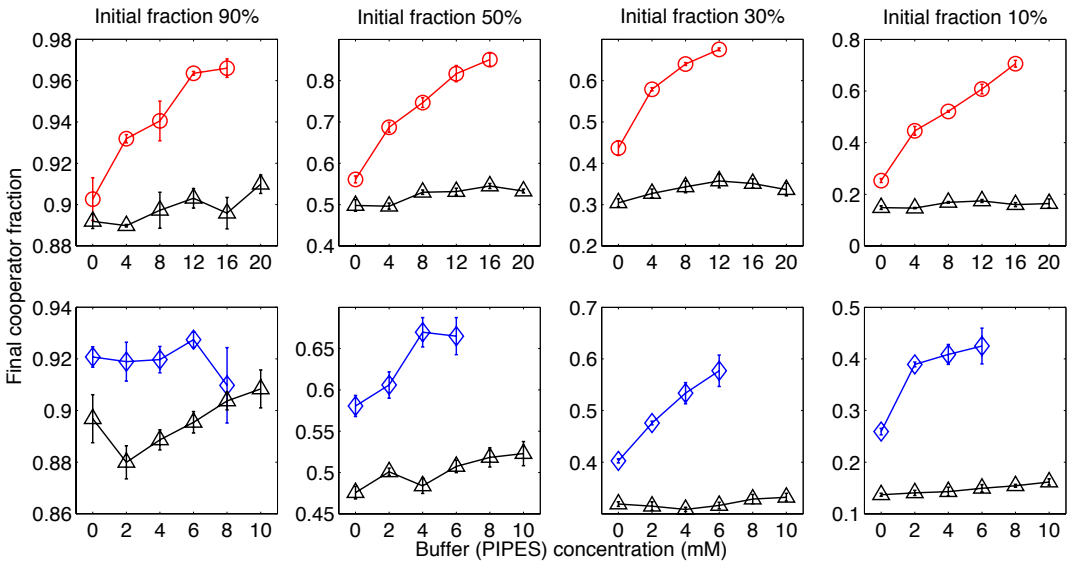

Figure S6: Competition between yeast and bacteria with different initial cooperator fractions. Each individual plot shows the final cooperator fraction (after 10 days of growth) as a function of buffer concentration in the media. Top row shows the results for competition between yeast and DH5α (circles) and the bottom row shows the results for competition between yeast and JM1100 (diamonds). In all the plots, pure yeast controls are shown in triangles. Note that when competing against DH5α, even starting with 90% initial cooperator frequency, cooperator fraction increased in most of the buffering conditions, suggesting that at equilibrium yeast population might consist of only cooperators. For experimental details see Methods. Error bars, ± s.e.m. (n = 3).

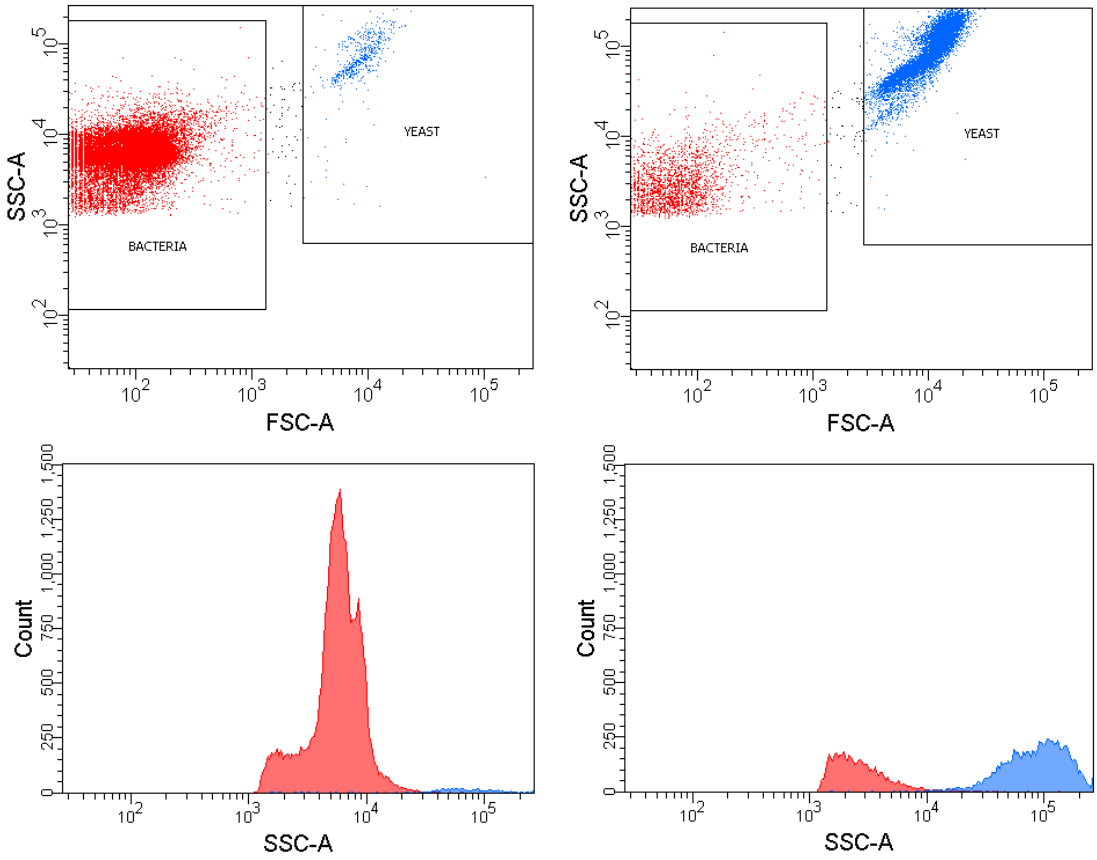

Figure S7: Bacterial density measurements using flow cytometry. Left column shows a typical bacterial density measurement from a two species competition culture. This particular sample is competition after 10 days of growth with 30% initial cooperator fraction and 12 mM buffer (PIPES). To collect the data, bacterial settings were used on the flow cytometer (see Methods). As seen in the top SSC/FSC plot, bacteria (red) and yeast (blue) populations were well separated and easily distinguished. Bottom plot shows the histogram SSC counts for the same condition. In this histogram, skewed left tail of the bacterial counts is due to noise overlapping with the bacterial population counts. To quantify the noise and subtract it from bacterial counts, every growth cycle we measured event counts occurring in the 'BACTERIA' gate for 8 pure yeast cultures (isolated yeast controls) again using the bacterial settings. Right column shows a typical result from such a measurement. This particular sample is from a culture after 10 days of growth with 30% initial cooperator fraction and 12 mM buffer (PIPES) – same as the conditions used in the left column except without bacteria. Top right plot shows SSC/FSC plot with noise appearing in the region where bacteria was before. In the SSC histogram for this sample (bottom right plot), we see that noise counts overlap nicely with the left tail of bacterial counts from the sample with bacteria (bottom left plot). Bacterial counts in mixed culture experiments were

corrected by subtracting the mean of such 8 controls from each sample for every different microplate measurement.

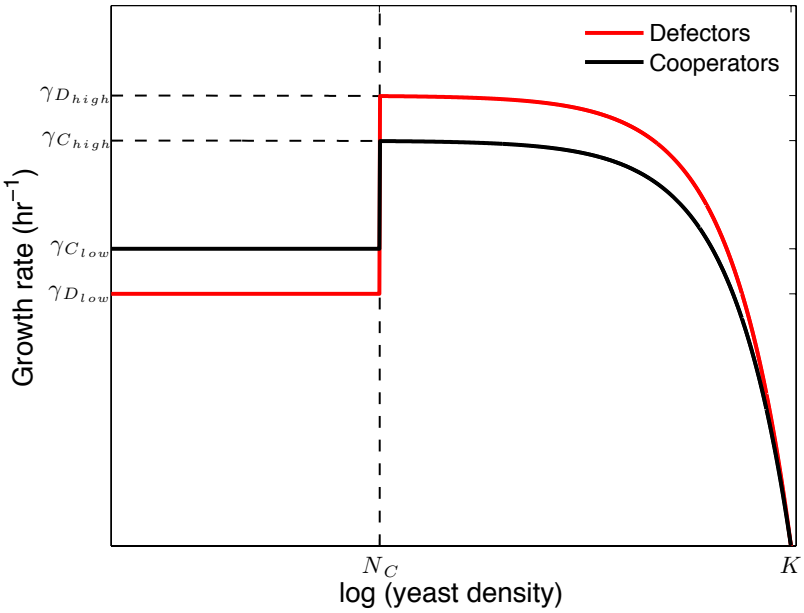

Figure S8: Two-phase logistic growth model. To model the cooperative dynamics within the yeast population, we developed a simple growth model based on experimental measurements. It has been shown that due to the cooperative nature of growth on sucrose, yeast growth rate is lower at low-density conditions and becomes higher as population density increases (Gore *et al*, 2009, Dai *et al*, 2012). We have measured the low-density and high-density growth rates of cooperating yeast populations (as reported below) and confirmed that this was indeed the case. This observation led us to develop a two-phase growth model whereby during the low-density conditions (initial stages of batch culture) yeast growth rate is lower compared to the later stages of the culture where the cell density is higher and faster glucose accumulation occurs. Furthermore, it was shown that when grown separately in low-density conditions, the cooperator growth rate was higher than cheater (defector) growth rate on media containing low glucose concentrations but high concentrations of sucrose (Gore *et al*, 2009). This result was expected, as cheater cells effectively cannot utilize sucrose, while cooperator cells can break down sucrose and capture some of produced products before they get diluted away in the well-mixed environment that was experimentally imposed. This conclusion was further supported by experiments in which we observed that if the dilution factor between successive cycles of batch growth was higher (>1,000) or cycle length was shortened (24 h instead of 48 h)—thereby imposing low-density conditions— cooperator frequency increased faster in mixed cultures of cooperator and cheater yeast cells. Therefore, we chose to assign a lower value to cheater growth rate at low-density conditions (described in detail below). Since our experiments are performed in batch culture, to

simulate the nutrient limited nature of the total growth and final biomass, we let yeast growth to be logistic. We have observed this sort of logistic growth dynamics consistently during our experiments whereby the yeast density saturated after a certain amount of time (Fig 2A, Fig S5A).

A sketch of this model shown in the above figure describes how the growth rate changes as a function of yeast density. At low density, cooperators have a higher growth rate ($\gamma_{C_{low}}$) than cheaters ($\gamma_{D_{low}}$). Above a yeast density N_C where cooperator density is at a critical value, it is assumed that the growth rate is higher for both cooperators and cheaters since glucose accumulates faster in the media(Gore *et al*, 2009). Then, the growth rate decreases logistically to zero as the yeast density reaches its carrying capacity, *K*. We measured the critical cooperator density at N_C to be about 3 x 10^5 cells/mL and $\gamma_{C_{low}}$ as 0.33 hr^{-1}. These measurements were taken by observing the time it took purely cooperative yeast cultures to reach a certain density, starting with different initial cell densities. Note that N_C is more than two orders of magnitude lower than final cell density that can be achieved by a pure yeast culture in our prepared media over 48 hrs (see K_{max} below). Therefore, we assumed growth rate below this yeast density to be approximately constant (no logistic decline). This assumption can be visualized on the above figure, where below N_C, on a log scale, projections of logistic lines can be taken to be not a function of yeast density as they are nearly constant. In other words, we can ignore the drop in nutrient concentration during the period in which yeast density reaches N_C, as this value is much lower compared to the final yeast density, therefore the nutrient depletion is only a small fraction of the total nutrients present in the media. $\gamma_{C_{high}}$ was measured to be 0.45 hr^{-1} on 4% sucrose by measuring growth rate during exponential growth. Taking the cost of cooperation into account, $\gamma_{D_{high}}$ was assigned such that $\gamma_{C_{high}}$ was 1% lower than $\gamma_{D_{high}}$ (Figure S1). Highest *K* value in a pure yeast culture on our default media was measured to be 15x10^7 cells/mL (K_{max}). To simulate nutrient limitation or competition with bacteria, *K* was varied across the experimentally observed range.

$\gamma_{D_{low}}$ (cheater growth rate at low density) was treated as a phenomenological parameter and was varied to fit the data shown in figure 3c. In nutrient limitation conditions, cheaters had a growth deficit of 4.85% at low density compared to cooperators. For JM1100 treatment, this deficit was 4.85% + 5.45% * (1– K/K_{max}) and for DH5α it was 4.85% + 13% * (1– K/K_{max}). These values were assigned so as to fit the data. We assumed that cheaters have a lower growth rate than

cooperators when competing against bacteria, because bacteria might compete for glucose with yeast and this would further limit the available glucose in the media during low-density conditions (yeast density $<N_C$). This model enabled us to calculate temporal dynamics and simulate the entire growth process over 5 cycles of growth (10 days) with 1:1,000 serial dilutions in between. Lower carrying capacity due to nutrient limitation or bacterial competition meant that the yeast population would spend more time during the first phase of this growth model where cooperation is favored. According to our model, equilibrium fraction of cooperators without the presence of bacteria is 61%.

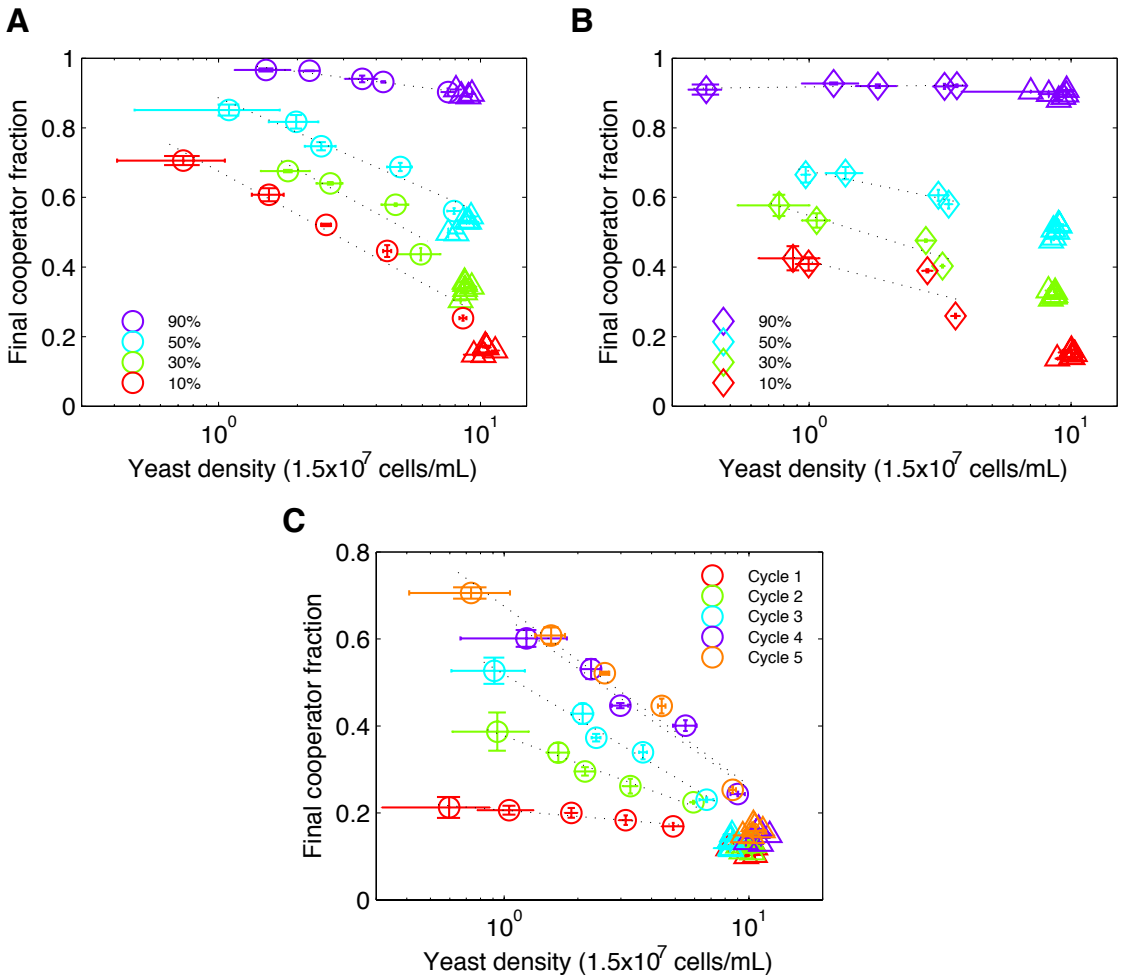

Figure S9: Log-linear relationship between yeast density and final cooperator fraction shown for different initial cooperator fractions (A, B) and different time points during experiments (C). **(A)** Competition results between yeast and DH5α with different initial cooperator fractions (circles) after 5 cycles. **(B)** Competition results between yeast and JM1100 with different initial cooperator fractions (diamonds) after 5 cycles. Triangles represent results for pure yeast cultures both in (A) and (B). **(C)** Final cooperator fraction within the yeast population over time while competing against DH5α. Each cycle is 48 hrs. Data points represent different buffering conditions. Yeast density decreases monotonically with buffering in all the plots above. Note the apparent increase in the final yeast density as the yeast population becomes more cooperative in (C). Dotted lines represent least squares fit for the data. Error bars, ± s.e.m. (n = 3).

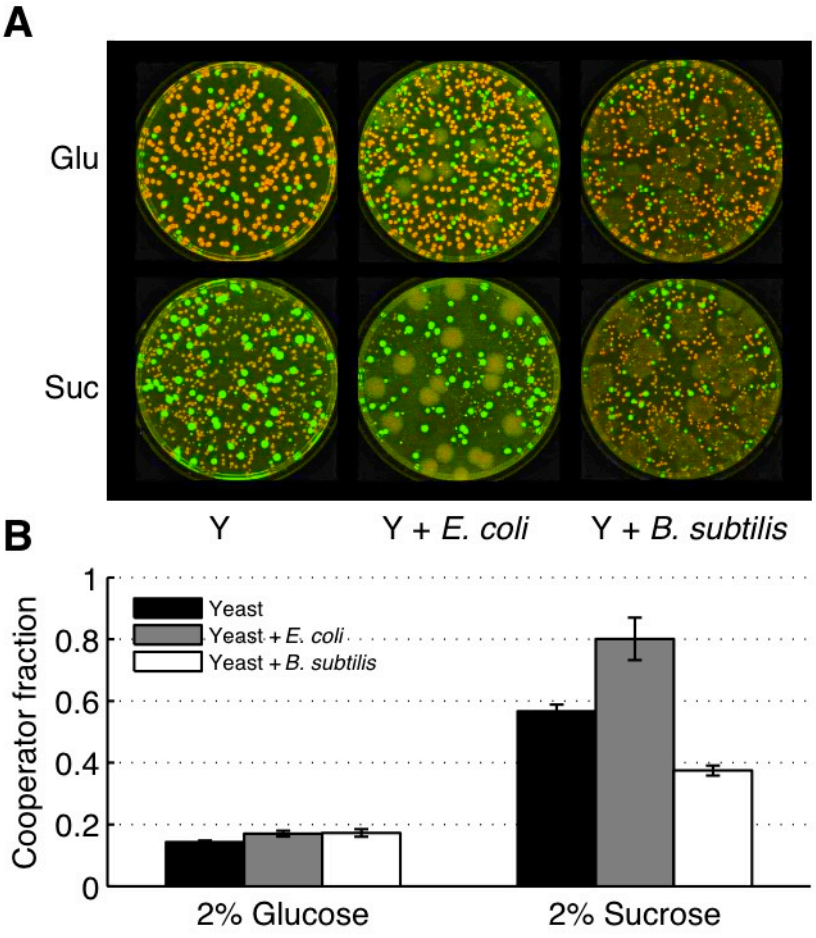

Figure S10: Competition against *E. coli* or *B. subtilis* on agar plates. Growth on agar plates of yeast only, yeast with *E. coli*, and yeast with *B. subtilis* **(A)** Images were taken after 4 days of growth at 30°C. Yeast (Y) was competed against either *E. coli* (JM1100) or *B. subtilis* on rich media plates (100mm diameter) supplemented with either 2% Glucose or 2% Sucrose. Cooperator yeast colonies appear yellow/green, cheater yeast colonies appear red and bacterial colonies appear dull colored and bigger compared to yeast colonies. **(B)** Colonies were washed off of imaged plates and yeast cooperator fractions were measured by flow cytometry. As expected, competition with *E. coli* selected for cooperators within yeast. In contrast, *B. subtilis* favored cheating. Error bars, ± s.e.m. (n = 3).

A **B**

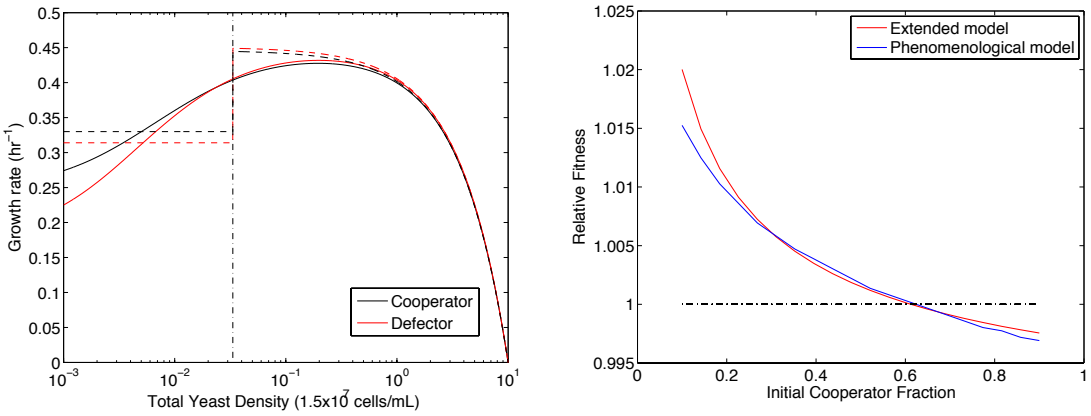

Figure S11: A detailed yeast growth model produces similar results as our phenomenological model: To show that our phenomenological model (Figure S8) can predict yeast growth dynamics accurately, we developed a logistic growth model incorporating glucose production by cooperator cells. In this extended model, the growth rates of cooperators (γ_C) and defectors (γ_D) were assumed to follow Monod-like dynamics as a function of the glucose concentration together with logistic growth at high cell density:

$$\gamma_C = \gamma_{C_0}\left(1-\frac{N}{K}\right)\left(\frac{G+g}{G+g+K_m}\right)$$

$$\gamma_D = \gamma_{D_0}\left(1-\frac{N}{K}\right)\left(\frac{G}{G+K_m}\right)$$

Here, γ_{D_0} is 0.45 hr^{-1} and γ_{C_0} is 0.99x0.45 hr^{-1} corresponding to the 1% fitness cost of producing invertase as used in the phenomenological model. N is the varying total yeast density during a batch culture and K (15x10^7 cells/mL) is the carrying capacity of the yeast population. Growth rate of yeast cells is assumed to be a function of G (which denotes the glucose concentration (%) in the media) with Michaelis-Menten (Monod) dynamics, where K_m is 0.005% to yield an approximately correct growth rate at low cell density. However, we note that previous measurements suggest that the growth rate saturates more rapidly with increasing glucose concentration than is assumed in the Monod / Michaelis-Menten form above (Gore et al, 2009). Initial G concentration is set to be 0.005%, as in our experiments. g denotes the small amount of glucose concentration felt and captured directly by the cooperator cells. g was set to be 0.003% as described in Gore et al.

We modeled the glucose production to be proportional to the cooperator cell density:

$$\frac{dG(\%)}{dt} = \frac{Cooperator\ density\left(\frac{cells}{L}\right)\ x\ 4.5x10^{8}\left(\frac{molecules}{\sec x\ cell}\right)}{N_A}\ x\ 180(\frac{g}{mol})\ x\ 0.1$$

Time step (dt) used in the simulations is 1 sec. Based on our previous measurements, we set the sucrose hydrolysis rate to be $4.5x10^{8}\left(\frac{molecules}{\sec x\ cell}\right)$ (Gore et al 2009). In this model we only explicitly consider glucose creation (not glucose consumption), as the primary dynamics between the cooperator and cheater yeast strains are determined by the glucose concentration at low cell density. As the cell density increases glucose and other resources will be exhausted, which is what leads to the logistic slow-down of cell division at high cell density. N_A is the Avagadro's number and 180 g/mol is the molecular weight of glucose. We multiply by 0.1 to convert g/L into % (w/v) concentration.

Using this model, we simulated the growth dynamics of mixed yeast cultures and compared the results to the predictions of our phenomenological model. (A) We found that growth rates of yeast strains as a function of yeast cell density behave qualitatively very similar to the phenomenological model. Moreover, we found that after a critical cooperator cell density, the cheater growth rate exceeds the cooperator growth rate, although at low-density conditions the cooperator growth rate is higher. This critical density was almost exactly the same for the extended model as the one used in our phenomenological model. For the parameters of the phenomenological model, we used exactly the same values given in Figure S8 (e.g. critical cooperator density was 3 x 10^5 cells/mL, cheater growth deficit at low density conditions was 4.85%). Starting cell densities were 1.5x10^5 cells/mL and initial cooperator fraction was 60% for the plots in (A).

Next, we simulated cultures with different starting cooperator fractions and plotted the relative fitness of cooperators as a function of starting cooperator frequency (B). We found that the results of the extended model were almost identical to the phenomenological model and both models predicted the equilibrium fraction of cooperators to be around ~60%. For these simulations, we used an initial yeast density of 1.5x10^6 cells/mL (equilibrium density during experiments with 1000x dilution). The relative fitness was calculated using the formula given in Figure S1. These results show that although simple, our phenomenological model captures the essential dynamics of yeast growth on sucrose accurately. In our simulations, by decreasing the initial glucose concentration, we can indeed drive the equilibrium fraction of cooperators to 1 (occurs at initial

glucose concentration of ~0.001%). This result shows that glucose consumption due to the presence of bacteria would drive the increase in cooperator fractions in this model.

In this mechanistic model we have attempted to use experimentally measured parameters together with well-known growth equations (i.e. Monod), meaning that the growth rates at low cell density are different in the mechanistic model and in our phenomenological model. Nevertheless, the primary argument that we are attempting to make here is that a mechanistic model which explicitly treats glucose concentration will yield similar predictions regarding cooperation/cheating as our phenomenological model that simply has two-phases of growth corresponding to low and high cell density. Figure S11B above argues strongly that the two modeling approaches make similar predictions.